Supplementary Information:

- **Supplementary Experimental Procedures**
- **Supplementary Figures S1 to S5**
- **Supplementary Movies S1 to S12**

Supplementary Information
Supplementary Experimental Procedures

Antibodies and reagents. The following antibodies were purchased from Santa Cruz Biotechnology: mouse anti-SQSTM-1/p62 (sc-28359) (was used for WB and IF staining), rabbit anti-SQSTM-1/p62 (sc-25575) (was used for IF co-staining in the presence of a mouse anti-α6 antibody), anti-HSP90α (sc-515081), anti-c-Myc (sc-40; used only for Western blotting), anti-UbcH5A/B/C (sc-166278), anti-Skp1 (sc-5281), anti-USP15 (sc-100629), and anti-USP26 (sc-51010). Mouse anti-FLAG antibody (F1804) and rabbit anti-FLAG antibody (F7425) (was used only for IF co-staining in the presence of an anti-α6 antibody) were from Sigma-Aldrich. Anti-active caspase-3 (ab13847), anti-beta actin (ab8224), anti-Fbxw7 (ab109617), anti-c-Myc (ab32076), and anti-Rbx1 (ab133565) antibodies were purchased from Abcam. Anti-HSP70 (4873), anti-GFP (2955) and anti-Cul1 (4995) antibodies were purchased from Cell Signalling Technologies. Anti-K48 (05-1307) and anti-K63 (05-1308) were purchased from Merck. Anti-HA tag (901503) antibody was from BioLegend. Anti-α6 hybridoma was purchased from the Developmental Studies Hybridoma Bank. Anti-Rpn1 antibody was kindly provided by Shigeo Murata (University of Tokyo). Anti-Ub conjugates (1) and anti-E1/UBA1 (2) antibodies have been described previously. Alexa Fluor-conjugated (488, 568, and 633) secondary antibodies (goat anti-mouse and anti-rabbit) were purchased from Invitrogen. Goat anti-Rat Alexa Fluor 647 (far-red) (4418) was purchased from Cell Signalling Technologies. Oligonucleotides were synthesized by Hylabs and Integrated DNA Technologies. CalFectin reagent for cDNA transfection was purchased from SignaGen Laboratories. Hoechst 33342 (bisBenzimide, B2261), 1,6-Hexanediol (240117), Arsenic trioxide (ATO, A1010), Leptomycin B (L2913), cycloheximide (CHX, C4859), DMSO (D2650), *N*-ethylmaleimide (NEM), iodoacetamide, puromycin and sucrose were purchased from Sigma-Aldrich. E1 inhibitor MLN-7243 (HY-100487) was purchased from MedChemExpress (MCE). Proteasome activity probe Me4BodipyFL-Ahx3Leu3VS (Bodipy probe, I-190-050) was purchased from R&D Systems. MG132 (474790) was purchased from Millipore. Hydrogen peroxide (H_2O_2) was purchased from Merck.

Cells culture and transfection. HeLa cervical carcinoma, A549 lung carcinoma, MCF7 and MDA-MB-231 breast carcinoma cells, and HEK293FT embryonic kidney cells (all human), were purchased from the American Type Culture Collection (ATCC). Cells were cultured in Dulbecco's Modified Eagle's medium (DMEM) (Biological Industries, Bet HaEmek, Israel) supplemented with 10% FBS (Gibco), sodium pyruvate (1 mM; Biological Industries), L-glutamine (2 mM; Biological Industries), and penicillin/streptomycin (100 U/ml and 0.1 mg/ml, respectively; Biological Industries) at 37^0C in a humidified atmosphere containing 5% CO_2. Transfection was carried out using the CalFectin transfection reagent according to the manufacturer's instructions. Transfection in 24-well plates was performed for live cell imaging (see also under *Live Cell Imaging* below).

Plasmids. cDNA encoding for FLAG-tagged SQSTM1/p62 and its deletion mutants FLAG-p62ΔPB1 (deletion of aa 1-123) and FLAG-p62ΔUBA (deletion of aa386-440), were reported in our previous study (3). cDNA encoding for K7R mutant of p62 was generated by replacing Lys7 with Arg using the

QuikChange™ Site-Directed Mutagenesis Kit (Agilent Technologies) according to the manufacturer's protocol. The following primers for generating the p62K7R point mutation were purchased from Hylabs: The forward and reverse oligonucleotides were CGCTCACCGTGAGGGCCTACCTTCTGGGC and GCCCAGAAGGTAGGCCCTCACGGTGAGCG, respectively. All four p62 constructs (FLAG-p62, FLAG-p62ΔPB1, FLAG-p62ΔUBA, and FLAG-p62K7R) served as templates to generate the corresponding deletion mutants of the NES domain (aa303-320). Primers for ΔNES mutation were purchased from Integrated DNA Technologies (IDT), and their sequences were: forward GTGGGAATGTTGAGGGCCGCCCTGAGGAACAGATG and reverse CATCTGTTCCTCAGGGCGGCCCTCAACATTCCCAC. The GFP-p62ΔNES construct was generated by fusion of p62ΔNES construct to EGFP in FUGWm vector (4). Specifically, the segment of p62ΔNES was cloned from the FLAG-p62ΔNES construct by PCR using two primers: forward ACTCTCGGCATGGACGAGCTGTACAAGGGCGGCGGCGGCAGTGCGTCGCTCACCGTGAAG and reverse TATCGATAAGCTTGATATCGTCACAACG GCGGGGGATG. FUGWm vector was cut with two restriction enzymes, BsrGI (5') and EcoRI (3'). PCR product of p62ΔNES was purified and inserted into the FUGWm vector downstream to EGFP using a NEBuilder HiFi DNA Assembly Cloning Kit (New England Biolabs). Purified GFP-p62ΔNES construct was introduced into p62KO HeLa cells using either 3rd generation lentiviral vector based on the FUGWm backbone, or via standard transfection reagents (see below under *Cell Culture and Transfection* and *Lentivirus production and transduction*). Expression vector encoding mRFP-Ub was purchased from Addgene (plasmid #11935; http://n2t.net/addgene:11935; RRID:Addgene11935) (5). cDNA encoding for HA-Ub was sub-cloned into the pCAGGS vector (4).

Lentivirus production and transduction. Lentiviral particles were produced by transfecting HEK293FT cells with a mixture of two packaging plasmids: ΔNRP, VSVG, and the appropriate expression vectors, including FUGWm-GFP-p62ΔNES, NSPI-NLS-GFP-CL1, NSPI-β4-GFP, and NSPI-RPN11-GFP (the last three were prepared using standard molecular biological methods). Transfection of HEK293FT cells was performed using the Calfectin reagent in 10 cm plates when cells had reached 70% confluence. Supernatants that contain lentiviral particles were collected 48 hours after transfection, passed through 0.45 μm filters, aliquoted, and stored at -80^{0}C or used immediately. Transduction of p62KO or HeLa cells with lentivirus was performed by adding 1 ml fresh DMEM containing 10 μg/ml polybrene along with 1 ml filtered supernatant to each well of a 6-well plate. Puromycin (5 μg/ml) was added to the cells transduced with NSPI vectors-derived lentiviruses to select stable cells. Six stable cell lines were generated using lentiviral vectors in this study: p62KO/GFP-p62ΔNES, p62KO/NLS-GFP-CL1, HeLa/NLS-GFP-CL1, p62KO/β4-GFP, HeLa/β4-GFP, and p62KO/Rpn11-GFP cells.

Immunofluorescence microscopy. Cells were seeded into Eppendorf Cell Imaging Plates with cover glass bottom (170 μm). Approximately 2.5-5.0×10^4 cells were seeded in each well of a 24-well plate or 0.5-1.0×10^4 cells were seeded in each well of a 96-well plate. For immunofluorescence staining, cells were

fixed with 4% paraformaldehyde (PFA) (Electron Microscopy Sciences), diluted in phosphate-buffered saline (PBS, pH 7.4) for 20 min at room temperature followed by extensive washing with PBS. Cells were then permeabilized and blocked at room temperature for 30 min with a blocking buffer in PBS that contains 5% goat serum and 0.3% Triton X-100. Primary antibodies were diluted in blocking buffer at the following dilutions and incubated with cells overnight at 4^0C: mouse anti-FLAG (1:500), mouse anti-p62 (1:200), rabbit anti-p62 (1:200), rabbit anti-c-Myc (1:200), rat anti-HSP70 (1:100), rabbit anti-HSP90 (1:100), mouse anti-α6 (1:20), rabbit anti-K48 (1:500), rabbit anti-K63 (1:500), rabbit anti-Rpn1 (1:200), rabbit anti-active caspase-3 (1:200), goat anti-E1/UBA1 (1:500), mouse anti-UbcH5A/B/C (1:50), rabbit anti-Cul1 (1:100), rabbit anti-Rbx1 (1:200), mouse anti-Skp1 (1:50), goat anti-USP26 (sc-51010), mouse anti-USP15 (1:50), and rabbit anti-Fbxw7 (1:500). Cells were washed extensively with PBS prior to incubation at room temperature for 30 min with the relevant secondary antibodies (at 1:500 dilution in blocking buffer). After washing with PBS, cells were further stained with 5 μg/ml Hoechst in PBS for 10 min and washed again. Immunofluorescence microscopy was performed using Zeiss LSM700 confocal microscope (Carl Zeiss, Oberkochen, Germany) equipped with four diode laser lines: 405nm, 488nm, 555nm and 639 nm, and with a 63x oil immersion objective lens. Analysis, quantification and fluorescence distribution profiling of the immunofluorescence images were performed using the Zen software. For fluorescence distribution tracing, a straight line was drawn across the area of interest in a single nucleus. The fluorescence intensity in the corresponding channels (488 for green and 555 for red) were measured along the line. Results were normalized to the largest intensity obtained in each channel and displayed as line profiling graphs. Fluorescence intensity was expressed in arbitrary units.

Fluorescence recovery after photo bleaching (FRAP). Live cell FRAP analysis was performed on a Zeiss LSM700 confocal microscope equipped with Plan-Apochromat 63x/1.40 NA oil DIC M27 objective. Nuclear p62 condensates were bleached in a circular 2 μm^2 regions of interest using 1 sec pulse of the 488 nm laser at 80% power. Images of fluorescence recovery were traced using 488 nm laser in 1% power at a resolution of 512 by 512 pixels with 4x scan zoom every second for 60 frames. The recovery curves were generated by the Zen software, and the curve plotting and fitting were processed with the GraphPad Prism software ver. 9.0 (Graphpad Software).

Live cell imaging. Cells were seeded into 24-well Eppendorf Cell Imaging Plate with a cover glass bottom (170 μm) at approximately $2.5\text{-}5.0\times10^4$ cells per well. Next day, cells were transfected with plasmids encoding the appropriate cDNAs (GFP-p62ΔNES, FLAG-p62ΔNES or RFP-Ub). Medium was replaced 6 h after transfection. To perform live cell imaging, plates were placed on an ImageXpress® Micro Confocal system (Molecular Devices) at 37^0C in a humidified atmosphere containing 5% CO_2 for 2 h prior to visualization. Live cell imaging was conducted with a 40x objective and a filter group containing two laser lines - Texas Red and FITC.

Three-dimensional imaging, reconstruction and analysis. Three-dimensional (3D) imaging was performed on a Zeiss LSM700 confocal microscope using the Z-stack function. Specifically, images were captured at a resolution of 1,440 by 1,440 pixels, using a 63x (NA 1.40) objective, and a z-step size of 0.38 µm for 20-25 sizes, which scanned the entire nucleus. 3D images were processed and analysed using an Imaris 9.5 software (Bitplane, South Windsor, CT, USA). Briefly, surfaces of nuclei were reconstructed from the signal of the Hoechst staining. These nuclear surfaces were applied to extract precise volume and nuclear signals from all other channels. To generate 3D reconstruction of nuclear p62 condensates, nuclear p62 extracted from the Hoechst surface was applied to create surfaces using similar methods as used for calculation of the nuclear surfaces. Volume greater than 0.1 μm^3 was set as a filter for p62 condensate surfaces. The surfaces of p62 in nuclei were applied to measure the number, volume, and the circularity of nuclear p62 condensates and their interaction with other proteins.

1,6-hexanediol treatment. 1,6-hexanediol was used to distinguish liquid-like and solid-like states of p62 condensates in the nucleus. To observe the disruption of p62 nuclear condensates in live cells, p62KO cells were transiently transfected with GFP-p62ΔNES and seeded in 24-well Eppendorf Cell Imaging Plates with $0.5\text{-}1.0\times10^4$ cells in each well. Prior to adding 1,6-HD, the plate was incubated on an ImageXpress® Micro Confocal system at 37^0C in a humidified atmosphere of 5% CO_2. Time lapse imaging were performed using a 40x objective and 1 min interval for 1h before adding 1,6-HD. To prepare 3.5% 1,6-HD solution, 35 mg 1,6-HD powder were dissolved in 250 µl complete DMEM and 750 µl sterile DD H_2O. That in order to dilute the culture medium 4-fold in order to reduce the osmolarity of the solution (6). The imaging program was paused for a while, and the culture medium in the well was replaced quickly with 3.5% 1,6-HD solution. After 5 min imaging, the imaging program was paused again, and the alcohol was removed and replaced quickly with a fresh culture medium to let cells recover for 1 h. To observe the disruption of endogenous nuclear p62 condensates in HeLa cells, fixation with 4% PFA was performed after treating the cells with 3.5% 1,6-HD for 5 min, and after additional recovery for 1 h. Fixed HeLa cells were then blocked and incubated with p62 antibody as described under *Immunofluorescence microscopy*.

Degradation of proteins. Cells were treated with 100 µg/ml of CHX for the indicated times. To inhibit proteasome activity, MG132 (20 µM) was added along with CHX for the entire duration of the experiment. Cells were then processed as described under *Immunofluorescence microscopy,* under *Live cell imaging,* and under *Cell lysates, immunoprecipitation, and Western Blotting*.

Cell lysates, immunoprecipitation, and Western Blotting. For co-immunoprecipitation and analysis of associated proteins, cells were washed with ice-cold PBS, and scraped into lysis buffer (50 mM Tris·HCl pH 7.4, 130 mM NaCl, and 0.5% Nonidet P-40) supplemented with freshly added Protease Inhibitor Mixture (Roche), 5 mM ATP (for maintaining 26S proteasome complex integrity), 10 mM iodoacetamide, and 5 mM NEM. Protein concentration was measured using the BCA assay according to the manufacturer's

instructions (Pierce). The suitable antibody was incubated with 25 µl of protein G-Sepharose for 1 h at 4^0C, washed, and then incubated (2 h at 4^0C) with the appropriate lysate (600 µg of total protein). Beads were washed five times with complete lysis buffer, extracted with sample buffer which was subjected to gel electrophoresis and immunoblotting as indicated. For direct visualization of proteins in cell lysates, 40 µg of protein were resolved via SDS/PAGE, transferred to nitrocellulose membrane, and immunoblotted with the appropriate antibodies. For immunoprecipitation and direct detection of ubiquitin conjugated proteins, cells were resolved in RIPA buffer (150 mM NaCl, 0.5% sodium deoxycholate, 50 mM Tris-HCl [pH 8], 0.1% SDS, and 1% NP-40) supplemented with freshly added Protease Inhibitor Mixture, 10 mM iodoacetamide, and 5 mM NEM.

Data analysis. Image analysis and quantification of 2D immunofluorescent images were performed using the Zen software. Image analysis and quantification of 3D immunofluorescent images were performed using the Imaris software. Image analysis and quantification of live cell imaging were performed using the ImageXpress Analysis Software. Quantification of Western blot data was performed using the ImageQuant TL image analysis software (GE Healthcare). Statistical analyses were performed using the GraphPad Prism9 software (GraphPad Software).

Legends to SI Figures:

Fig. S1. Phase separation of nuclear p62 is mediated by its interaction with poly-ubiquitinated substrates. ***(A)*** Immuno-staining of p62 in WT, p62KO, and p62KO+WTp62 and p62KO+p62ΔNES Hela cells. ***(B)*** Quantitative analysis of the effect of LMB on formation of nuclear p62 condensates. The indicated cells were treated with either DMSO or LMB, and the number *(i)* and size *(ii)* of nuclear p62 foci were calculated from the nuclear portion of p62 (the images from which the data were derived are presented in Figure 1B). ***(C)*** Disruption of nuclear p62 condensates in HeLa cells by 1,6-HD. *(i)* Cells were treated with 1,6 HD and were allowed to recover as described under *Experimental Procedures*. They were then stained with mouse anti-p62. Nuclear p62 was extracted from the 3D nuclear reconstruction using the Imaris software (as described under *Experimental Procedures*); *(ii)* Circularity of p62 condensates in HeLa cells was measured from 3D images of control cells (Panel *Ci*) using the Imaris software. ***(D)*** Inhibition of ubiquitin conjugation to target substrates by the ubiquitin-activating enzyme (E1/UBA1) inhibitor MLN-7243 (5 μM). ***(E)****(i)* CHX treatment decreases the level of Ub conjugates in cells which is prevented by MG132; *(ii)* IF staining of HeLa cells for p62 and K48-based Ub chains following CHX and MG132 treatment. ***(F)****(i)* Ubiquitinated proteins bearing K48-based Ub chains are recruited to p62ΔNES condensates; (*ii* and *iii*) Intensity tracings (along dashed arrows) of K48 and p62 of the enlarged indicated frames taken from the p62KO cells in the presence *(ii)* or absence *(iii)* of FLAG-p62ΔNES. ***(G)(i)*** Recruitment of K63-based Ub chains to p62ΔNES condensates; *(ii)* Intensity tracing (along the dashed arrow) of p62 and K63.

Fig. S2. The UBA domain of p62ΔNES is required for its interaction with ubiquitinated proteins. ***(A)****(i)* Binding of K48- and *(ii)* K63-based Ub chains to nuclear p62. Deletion of the UBA domain of p62ΔNES abolishes almost completely its interaction with both types of chains, while deletion of the PB1 domain abolishes the interaction partially. Total amount of K48- *(iii)* and K63- *(iv)* based Ub chains in cells. The blots depicted in panels i and ii were carried out on the same membrane following stripping of the first antibody. Same is true for the blots depicted in panels *iii* and *iv*. ***(B)*** The ΔPB1 and ΔUBA mutants of p62ΔNES do not support foci formation. Same is true for p62ΔNES-K7R. ***(C)*** Co-localization of nuclear p62 with the deubiquitinating enzymes (DUBs) USP15 and USP26.

Fig. S3. Unincorporated excess of the β4-GFP proteasomal subunits are recruited to the p62ΔNES condensates and degraded there by an intact, β4-containing proteasome complex. ***(A)*** Proteasomal degradation of free β4-GFP subunits in p62 condensates was monitored following CHX treatment. Note the stable proteasome-incorporated β4-GFP subunit that is located to the outer shell of the p62 foci (last column, third panel from top). ***(B)*** p62 stimulates the degradation of free β4-GFP, but a certain fraction remains stable even after 20 h. ***(C)*** The UBA domain of p62ΔNES is necessary for its interaction with unincorporated (apparently ubiquitinated) β4-GFP.

Fig. S4. Oxidative, heat, and osmotic stress increase nuclear p62 phase separation in a Ub chains-dependent manner. ***(A)*** Heat treatment *(i)* and ATO *(ii)* increase ubiquitination in cells. ***(B)****(i)* Oxidative, heat and osmotic stress increase the number of nuclear p62 condensates in Hela cells. 3D imaging was performed and nuclear p62 fraction was extracted from the 3D nuclear reconstruction using the Imaris software (as described under Figures 1B and S1B)); *(ii)* Quantification of the data presented in panel Bi (p62 in ~30 cells was quantified for each condition; ****p<0.0001). ***(C)*** Stress-induced formation of p62 condensates requires active E1. *(i)* Live cell images of cells that were subjected to either oxidative or heat stress in the absence (DMSO; upper line) or presence (lower line) of the E1 inhibitor MLN-7243; *(ii)* Quantitative analysis of the number of p62 foci in cell nuclei (calculated from the images presented in *Ci*). The number of p62 foci in nuclei was calculated from 40-90 cells using the ImageXpress analysis software; ****p<0.0001. ***(D)****(i)* Sucrose-induced osmotic stress promotes p62-independent LLPS of the proteasome and its possible subsequent fusion with similarly induced but p62-containing condensates; *(ii)* and *(iii)* Intensity tracings of α6 and p62 (along the dashed arrows) of the enlarged indicated frames taken from the FLAG-p62ΔNES-reconstituted p62KO *(ii)*, and p62KO cells *(iii)*. ***(E)****(i)* Sucrose-induced osmotic stress condensates that are p62-independent recruit only K48-based ubiquitin chains (1st and 3rd lines), whereas those that are p62-dependent recruit – in addition – also K63-based chains (2nd and 4th lines); *(ii)-(v)*, Intensity tracings of the different condensates described under panel *(i).*

Fig. S5. C-Jun and its targeting UPS components are localized to nuclear p62 foci. p62 in nuclear foci co-localizes with c-Jun and SCF^{Fbxw7} E3 ligase complex (which contains Rbx1, Cullin1, Skp1, and the F-box protein Fbxw7) that catalyses ubiquitination of c-Jun.

Legends to supplementary Movies

Movie S1. p62 phase separation in HeLa cells under basal conditions. HeLa cells were cultured in the presence of DMSO for 4 h. After fixation, cells were stained with p62 antibody (white) and Hoechst 33342 (blue). 3D imaging and reconstruction were performed as described under *Experimental Procedures***.** Condensates of p62 in the nucleus were visualized and zoomed in to display the details of the 3D information. Simulation of rotation, signal on/off, and zoom in, were generated using the Imaris software and further edited with Windows movie maker.

Movie S2. p62 phase separation in HeLa cells following LMB treatment. HeLa cells were cultured in the presence of LMB for 4 h. Following treatment, cells were processed for analysis as described under Movie S1.

Movie S3. p62 phase separation disruption by 1,6-HD. p62KO cells were transfected with GFP-p62ΔNES. Cells were treated with 1,6-hexanediol (1,6-HD) for 5 min followed by replacement of the drug with fresh culture medium for additional 2 h. Time-lapse images were captured every 1 min during the 1,6-HD treatment and every 3 min during the recovery. Movies were generated by the ImageXpress software.

Movie S4. Fusion of p62 condensates under basal conditions. p62KO cells were transfected with GFP-p62ΔNES. Time-lapse images were captured at 5 min intervals for 24h. Images showing fusion of p62 foci were selected to generate this movie using the ImageXpress software.

Movie S5. Fusion of p62 condensates during cell recovery from 1,6-HD disruption. p62KO cells were transfected with GFP-p62ΔNES. Experimental set up was similar to that described under Movie S3. Time-lapse images were captured every 1 min for 2 h along the recovery period. Movies were generated using the ImageXpress software.

Movie S6. Visualization of p62 and the proteasome in the shell of p62 condensates. p62KO cells were transfected with p62ΔNES and stained with anti-α6 (green) and anti-p62 (red) antibodies. Z-stack images were captured with a step size of 0.38 µm. 25 z-stack images were processed using the ImageXpress software to generate the 3D simulation.

Movie S7. Degradation of NLS-GFP-CL1 in p62 condensates. p62KO cells stably expressing NLS-GFP-CL1 (left panel) or - in addition - transiently transfected with p62ΔNES (right panel), were treated with CHX (100 µg/ml) for 2 h. Time-lapse images were captured every 5 min for 2 h. Movies were generated using the ImageXpress software and edited by the Wondershare Filmora software.

Movie S8. Degradation of β4-GFP in p62 condensates. p62KO cells stably expressing β4-GFP were treated with CHX (100 μg/ml). Time-lapse images were captured every 5 min for 10 h. Movies were generated using the ImageXpress software.

Movie S9. Degradation of Rpn11-GFP in p62 condensates. p62KO cells stably expressing Rpn11-GFP were treated with CHX (100 μg/ml). Time-lapse images were captured every 5 min for 3 h. Movies were generated using the ImageXpress software.

Movie S10. Oxidative stress induced by arsenic trioxide stimulates p62 phase separation. p62KO cells stably expressing GFP-p62ΔNES were exposed to arsenic trioxide (ATO, 2 μM, 2 h). Live cell imaging was started immediately after the addition of ATO. Time-lapse images were captured every 3 min for 2 h. Movies were generated using the ImageXpress software.

Movie S11. Oxidative stress induced by hydrogen peroxide stimulates p62 phase separation. p62KO cells stably expressing GFP-p62ΔNES were exposed to hydrogen peroxide (H_2O_2, 200 μM, 2 h). Live cell imaging was initiated immediately after the addition of H_2O_2. Time-lapse images were captured every 3 min for 2 h. Movies were generated using the ImageXpress software.

Movie S12. Heat stress stimulates p62 phase separation. p62KO cells stably expressing GFP-p62ΔNES were exposed to heat stress (HS, 43^0C, 1 h + 37^0C, 2 h). Live cell imaging was started immediately after the heat treatment. Time-lapse images were captured every 3 min for 2 h. Movies were generated using the ImageXpress software.

Supplementary Information References:

1. Braten O, et al. (2016) Numerous proteins with unique characteristics are degraded by the 26S proteasome following monoubiquitination. *Proc Natl Acad Sci U S A* 113(32):E4639-47.

2. Mayer A, Siegel NR, Schwartz AL, Ciechanover A (1989) Degradation of proteins with acetylated amino termini by the ubiquitin system. *Science (80-)* 244(4911):1480–1483.

3. Cohen-Kaplan V, et al. (2016) p62- and ubiquitin-dependent stress-induced autophagy of the mammalian 26S proteasome. *Proc Natl Acad Sci U S A* 113(47):E7490–E7499.

4. Hitoshi N, Ken-ichi Y, Jun-ichi M (1991) Efficient selection for high-expression transfectants with a novel eukaryotic vector. *Gene* 108(2):193–199.

5. Bergink S, et al. (2006) DNA damage triggers nucleotide excision repair-dependent monoubiquitylation of histone H2A. *Genes Dev* 20(10):1343–1352.

6. Kroschwald S, Maharana S, Simon A (2017) Hexanediol: a chemical probe to investigate the material properties of membrane-less compartments. *Matters* 3(5):e201702000010.

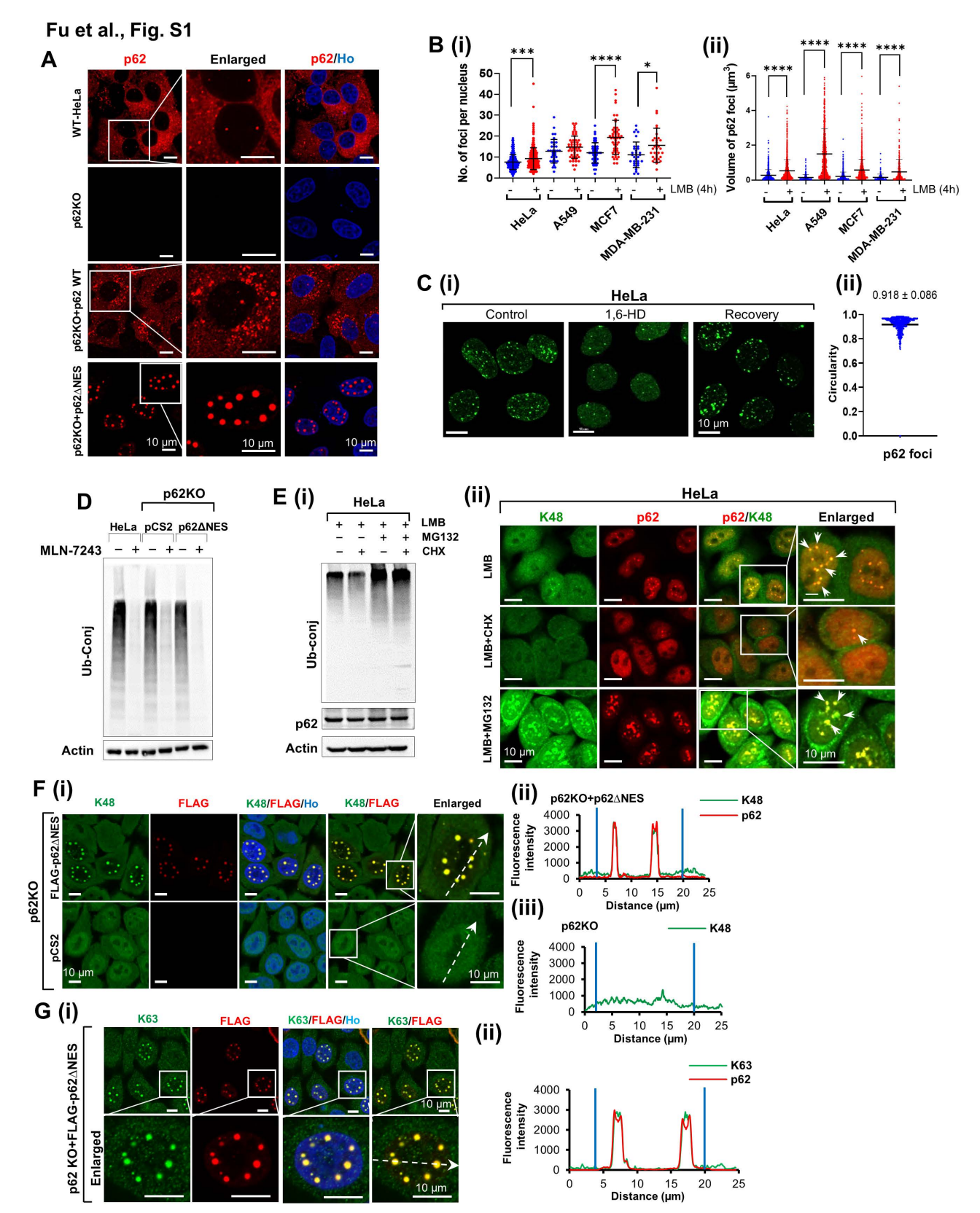
Fu et al., Fig. S1
A
p62
Enlarged
p62/Ho
WT-HeLa
p62KO
p62KO+p62 WT
p62KO+p62ΔNES
10 μm
B (i)
No. of foci per nucleus
***
****
*
LMB (4h)
HeLa
A549
MCF7
MDA-MB-231
(ii)
Volume of p62 foci (μm3)
C (i)
HeLa
Control
1,6-HD
Recovery
(ii)
0.918 ± 0.086
Circularity
p62 foci
D
p62KO
HeLa
pCS2
p62ΔNES
MLN-7243
Ub-Conj
Actin
E (i)
HeLa
LMB
MG132
CHX
Ub-conj
p62
Actin
(ii)
HeLa
K48
p62
p62/K48
Enlarged
LMB
LMB+CHX
LMB+MG132
F (i)
K48
FLAG
K48/FLAG/Ho
K48/FLAG
Enlarged
p62KO
FLAG-p62ΔNES
pCS2
(ii)
p62KO+p62ΔNES
Fluorescence intensity
Distance (μm)
(iii)
p62KO
G (i)
K63
FLAG
K63/FLAG/Ho
K63/FLAG
p62 KO+FLAG-p62ΔNES
Enlarged
(ii)

Fu et al., Fig. S2

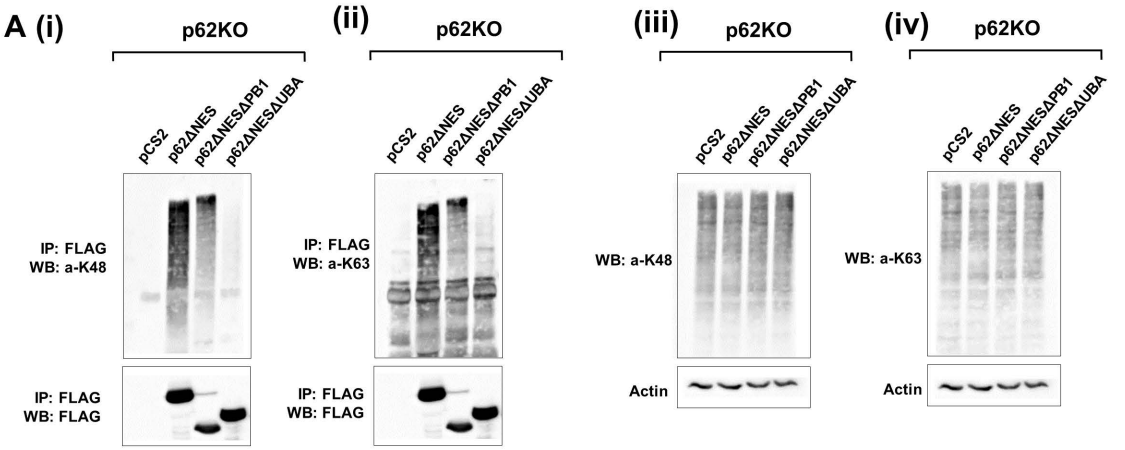

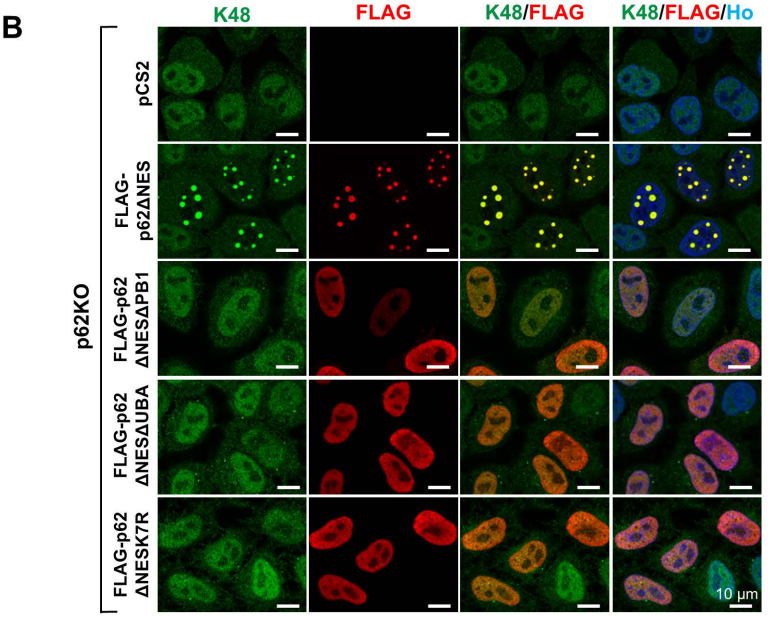

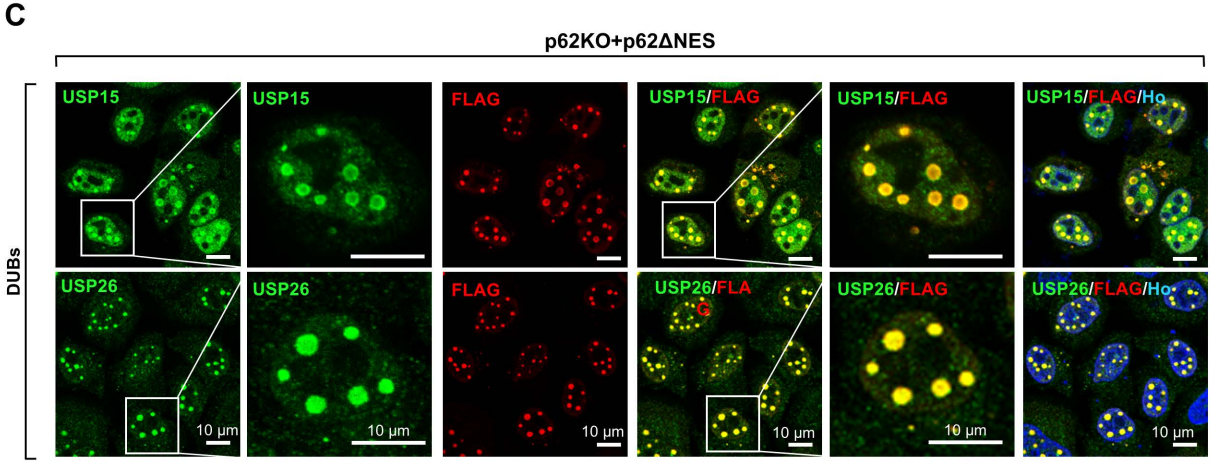

Fu et al., Fig. S3

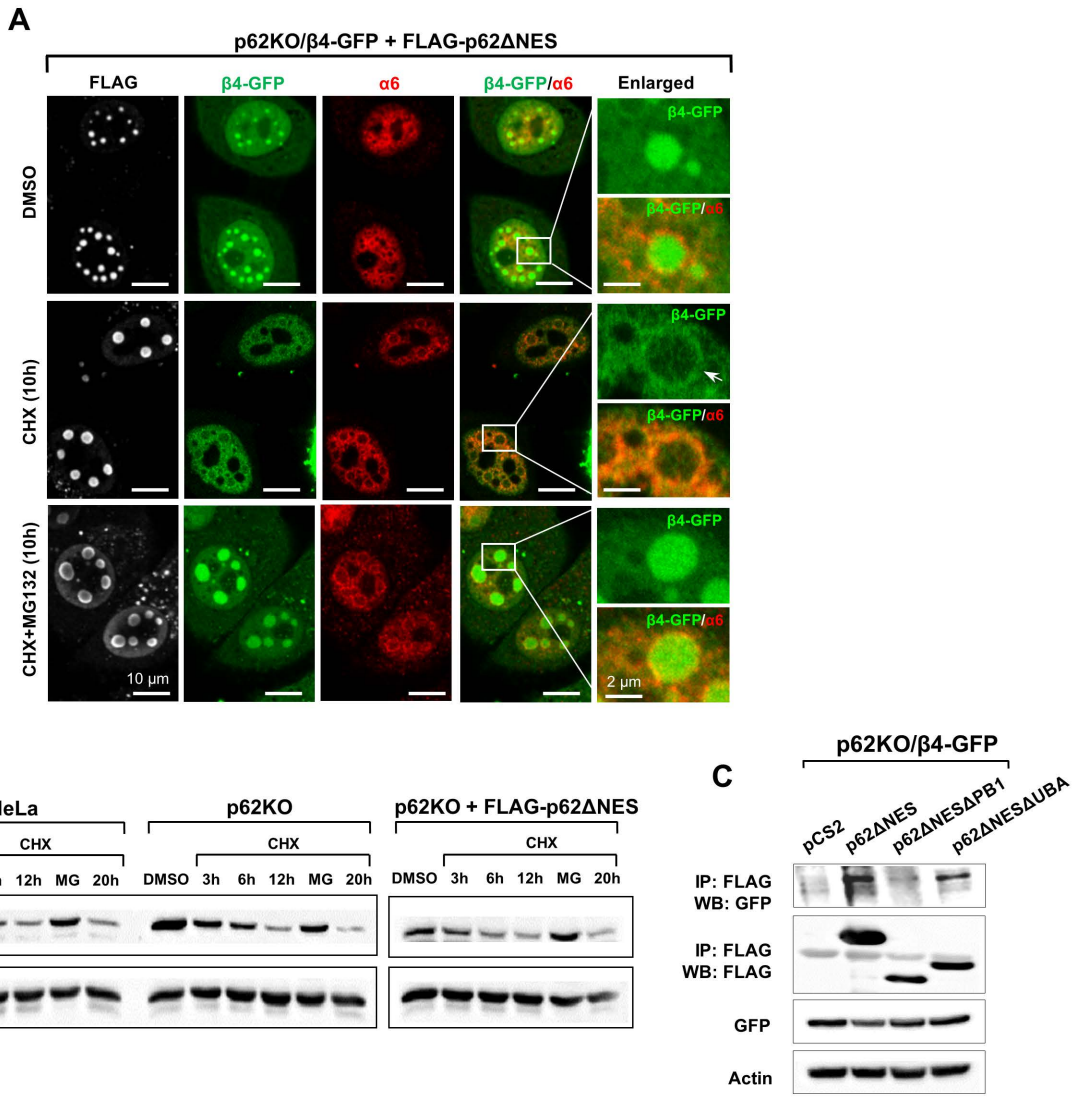

Fu et al., Fig. S4

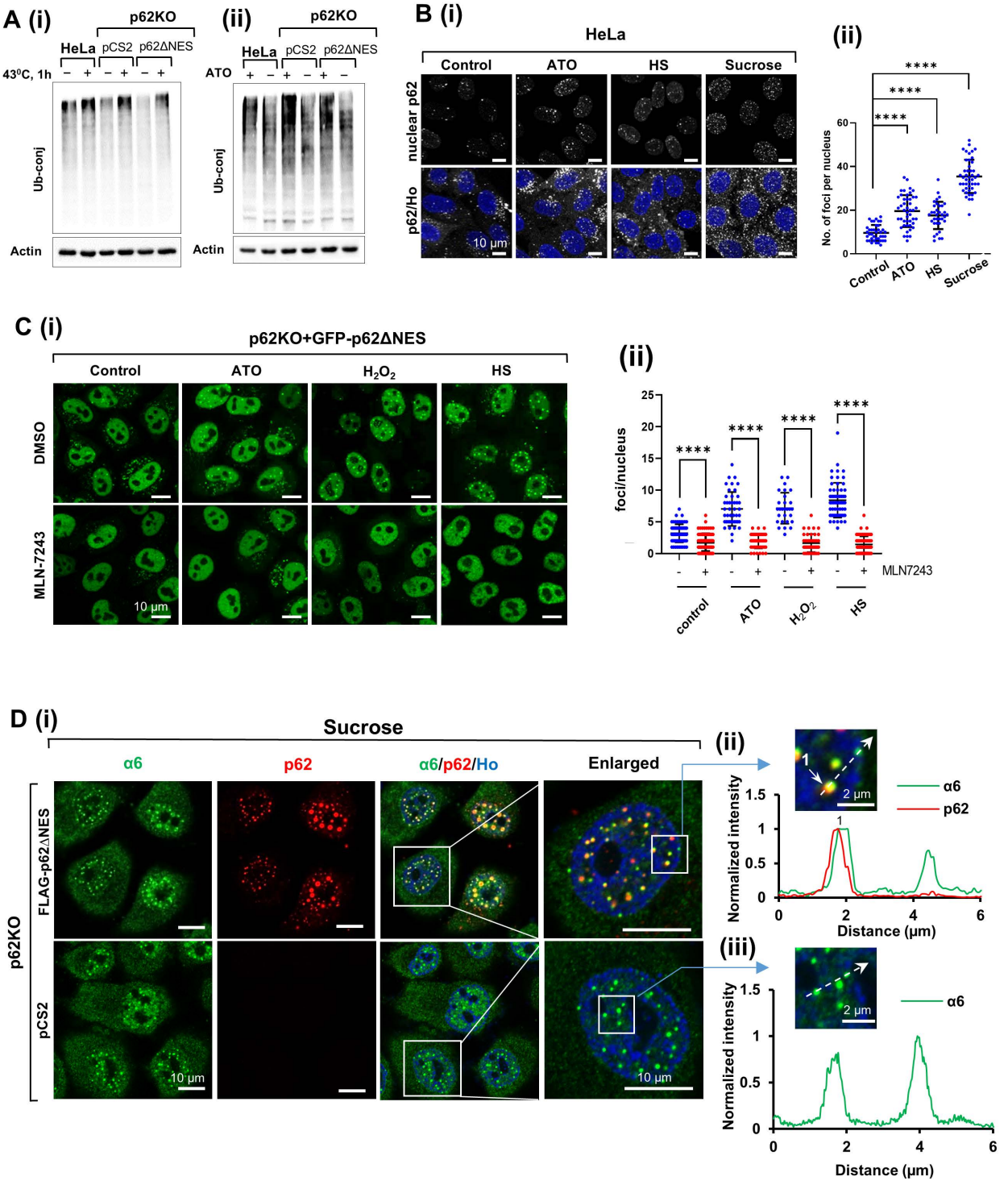

Fu et al., Fig. S4E

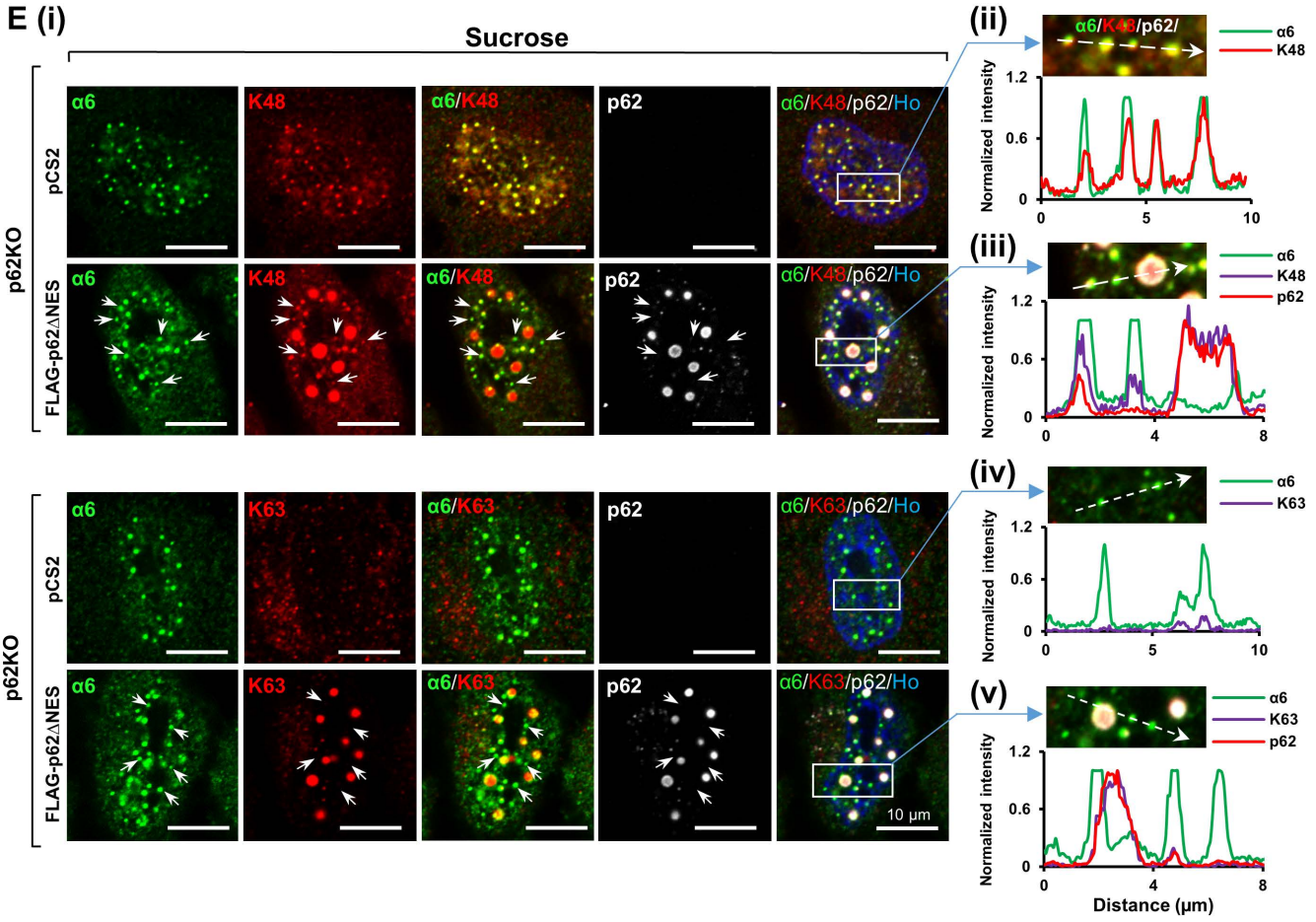

Fu et al., Fig. S5